

A PREDICTION OF OBSERVABLE ROTATION IN THE ICM OF ABELL 3266

KURT ROETTIGER

*Department of Physics and Astronomy
University of Missouri-Columbia
Columbia, MO 65211
E-mail: kroett@hades.physics.missouri.edu*

RICARDO FLORES

*Dept. of Physics and Astronomy
University of Missouri-St. Louis
St. Louis, MO 63121-4499
E-mail: Ricardo.Flores@umsl.edu*

Accepted for publication in the Astrophysical Journal

ABSTRACT

We present a numerical Hydro+N-body model of A3266 whose X-ray surface brightness, temperature distribution, and galaxy spatial and velocity distribution data are consistent with the A3266 data. The model is an old (~ 3 Gyr), off-axis merger having a mass ratio of $\sim 2.5:1$. The less massive subcluster in the model is moving on a trajectory from southwest to northeast passing on the western side of the dominant cluster while moving into the plane of the sky at ~ 45 degrees. Off-axis mergers such as this one are an effective mechanism for transferring angular momentum to the intracluster medium (ICM), making possible a large scale rotation of the ICM. We demonstrate here that the ICM rotation predicted by our fully 3-dimensional model of A3266 is observable with current technology. As an example, we present simulated observations assuming the capabilities of the high resolution X-ray spectrometer (XRS) which was to have flown on *Astro-E*.

Subject headings: Hydrodynamics— methods: numerical— galaxies: intergalactic medium — galaxies: clusters: individual (Abell 3266)—X-rays: Techniques: Spectroscopy

1. Introduction

A3266 is a nearby ($z=0.059$; Quintana, Ramirez & Way 1996), X-ray luminous cluster which exhibits optical and X-ray substructure. Two models have recently been proposed to explain the substructure in this cluster. Flores, Quintana, & Way (1999) have proposed that A3266 experienced a major merger *into* the plane of the sky while Henriksen, Donnelly, & Davis (1999) have proposed a minor merger parallel to the plane of the sky. Using a large sample of galaxy redshifts (387 galaxies), Quintana et al. (1996) suggested that A3266 might have experienced a merger 1-2 Gyr ago. Flores et al. (1999) found support for this interpretation using a simple N-body model. They noted an enhancement of galaxies north of the X-ray core similar, both visually and statistically, to the N-body particle spray found in their numerical simulations. They also noted a similar enhancement of emission-line galaxies in the same region. It has long been suggested that galaxies passing through cluster cores could be spectroscopically altered (Dressler & Gunn 1983), although it now appears that this would be mostly due to the tidal force rather than ram pressure by the ICM (e.g., Moore et al. 1996; Bekki 1999; Fujita et al. 1999). Burns et al. (1994) have suggested that the Coma cluster E+A galaxies distributed in the core and SW toward the NGC 4839 group are the result of a burst of star formation induced by a merger about 2 Gyr ago, which appears consistent with their starburst age (Caldwell et al. 1996). Similarly, the emission-line galaxies in A3266 could be the tail end of the disrupted less massive cluster in this model.

Evidence of recent dynamical evolution is also apparent in the X-ray surface brightness (XSB; Fig. 1) and temperature distributions. For example, the XSB was shown to exhibit a systematic centroid shift by Mohr, Fabricant & Geller (1993). Also, the XSB exhibits changing ellipticity and isophotal twisting between $4'$ and $8'$ (Mohr et al. 1993) as well as a large (~ 500 kpc) core radius (Mohr, Mathiesen & Evrard 1999), as would be expected in the case of a recent merger (Roettiger et al. 1996). Peres et al. (1998) find no evidence of a cooling flow. Several researchers (e.g., McGlynn & Fabian 1984) have suggested that mergers will disrupt cooling flows. Gómez et al. (1999) have demonstrated using numerical simulations that the time scale for re-establishment of the disrupted cooling flow in the post-merger envi-

ronment can be greater than several billion years, depending on the initial cooling flow and merger parameters. Markevitch et al. (1998; hereafter MFSV98) and Henriksen et al. (1999; hereafter HDD99) have produced temperature maps based on *ASCA* data that show significant temperature variations across the cluster. MFSV98 shows a radially decreasing temperature profile ranging from 12 keV in the central $3'$ to ~ 6 keV at radii greater than $8'$. De Grandi & Molendi (1999) find a similar radial temperature gradient using *BeppoSAX* data. The HDD99 temperature map exhibits a comparable range in ICM temperatures with a gradient increasing from NE to SW across the cluster.

In this paper, we extend the N-body model of Flores et al. (1999) by including the hydrodynamics of the ICM. We then demonstrate using a fully 3-dimensional numerical model that the current A3266 data are consistent with an old off-axis merger occurring largely *into* the plane of the sky. Off-axis mergers are a natural consequence of large-scale tidal torques, the latter being a generic feature of hierarchical clustering (Peebles 1969). The model of Flores et al. (1999) resulted in an off-axis merger as a result of the global angular momentum imposed at the protocluster stage, which in terms of the standard dimensionless angular momentum λ (Peebles 1969) corresponded to $\lambda = 0.07$. This amount is consistent with tidal torquing and is expected to be largely independent of mass (Barnes & Efstathiou 1987). Therefore the characteristics of the merger are not sensitively dependent on extending the region that was simulated around the cluster. In sufficient quantity, angular momentum can significantly alter the internal structure of clusters, which can then influence our interpretation of other cluster observations. As an example, numerical simulations (Inagaki et al. 1995; Roettiger et al. 1997) have shown that the shape of clusters (e.g., oblateness being a consequence of rotation) can have significant systematic effects on determinations of H_0 based on the Sunyaev-Zeldovich effect (see Birkinshaw (1999) for a review).

We describe our model and make direct comparisons to the data in §2. In §3, we present detailed models of proposed *Astro-E* observations based on the line-of-sight (LOS) ICM density, temperature and velocity structure provided by the numerical model. Section 4 is a summary of our results. We assume $H_0 = 70 \text{ km s}^{-1} \text{ Mpc}^{-1}$ when scaling the simulation to physical dimensions.

2. A Numerical Model of A3266.

We have created a numerical model of A3266 using the same technique that we have employed in several previous models of specific Abell clusters (e.g., A2256 Roettiger et al. 1995; A754, Roettiger et al. 1998; A3667, Roettiger, Burns & Stone 1999). Within the framework of idealized initial conditions, we survey merger parameter space (mass ratios, impact parameters, gas content, etc.) using a fully 3-dimensional Hydro/N-body code based on the Piecewise-Parabolic Method (PPM; Colella & Woodward 1984) and a Particle-Mesh (PM) N-body code. We then attempt to maximize agreement between synthetic observations of the simulation and various cluster observables (X-ray surface brightness, X-ray temperature distribution, galaxy spatial and velocity distributions etc.) in order to constrain not only the merger parameters, but also the epoch and viewing geometry of the merger. Here, we have modeled A3266 as an off-axis merger between a primary cluster of $\sim 1.1 \times 10^{15} M_{\odot}$ and a secondary of $\sim 5 \times 10^{14} M_{\odot}$ in which closest approach occurred approximately 3 Gyr ago. The secondary cluster, moving southwest to northeast, passed to the west of the primary cluster's core at a distance of ~ 230 kpc with a velocity of ~ 2500 km s $^{-1}$. The trajectory is believed to be into the plane of the sky at an angle of $\sim 45^{\circ}$.

Figure 2 shows the synthetic XSB image generated from the model. Like the *ROSAT* PSPC image (Fig. 1), the simulated image shows a generally spherical distribution at large radii with significant isophotal twisting near the X-ray core which is elongated NE to SW. The orientation of the X-ray cores (both simulated and observed) are not well-aligned with the projected mass distribution derived from gravitational lensing (Joffe et al. 1999) further indicating that the cluster is not fully relaxed. It should be noted that the resolution of the numerical simulations (~ 75 kpc or ~ 4 zones core radius) is significantly less than the resolution of the *ROSAT* image ($15''$ /pixel or $\sim 20 h_{70}^{-1}$ kpc).

Also included in Fig. 2 is a sampling of ~ 300 N-body particles ($< 1\%$ of total) from both the primary (\diamond) and secondary (+) clusters. The excess of secondary cluster particles to the north of the X-ray core accounts for the galaxy excess as well as the distribution of emission-line galaxies noted by Flores et al. (1999). The observed galaxy velocity distribution is indistinguishable from Gaussian within

the central region. The observed skewness and kurtosis within the central $1^{\circ} \times 1^{\circ}$ field are 0.024 and 0.14, respectively, while the N-body particle values are 0.051 ± 0.15 and 0.13 ± 0.26 . On a larger scale ($\sim 2^{\circ}$), Flores et al. (1999) find the observed skewness and kurtosis to be 0.106 and 0.341, respectively. The global N-body velocity dispersion is 905 ± 40 km s $^{-1}$, while Quintana et al. (1996) observe a global galaxy velocity dispersion of 1085 ± 51 km s $^{-1}$. The discrepancy here is possibly due to choosing too low a value for the initial cluster β -parameter.

A3266 contains a central dumb-bell galaxy with a velocity separation of ~ 400 km s $^{-1}$. Quintana et al. (1996) suggest that this is consistent with the merger geometry proposed here. Although consistent with a younger merger that is nearly in the plane of the sky, it is also consistent with an older merger at any projection since the time scales for dynamical friction to act on the dominant galaxy are long (Kravtsov & Klypin 1998). The velocity separation noted here should be contrasted with the 2635 km s $^{-1}$ separation observed between dominant galaxies in the proposed young merger A2255 (Burns et al. 1995).

It has been suggested that radio source morphology may give clues to the ICM dynamics. The radio emitting plasma is believed to be 10 to 100 times less dense than the surrounding thermal gas making it susceptible to pressure gradients and flows within the ICM (e.g., Burns 1998). HDD99 used the morphology of two radio sources to support their model, and depending on the exact location of these sources within the cluster, they are also consistent with the model presented here. We should comment however that considerable caution must be used when interpreting radio source morphology in this context. Both sources in question are located SW of the cluster core (see Jones & McAdam 1992). One appears to be a head-tail source while the other is identified as a possible Wide-Angle Tailed radio source (WAT). WATs have been used as indicators of bulk flows in clusters, because they have traditionally been associated with central dominant galaxies which are presumed to be at rest in the cluster's gravitational potential minimum making knowable its exact location (and relative velocity) within the cluster. Consequently, any bending of the WAT tails is the result of ICM dynamics rather than motion of the host galaxy. However, both of these radio sources are associated with galaxies having velocities significantly different ($\Delta V \sim 800$ km s $^{-1}$) from the mean cluster velocity indicating

that they may have considerable velocities of their own and may even be foreground or background objects.

Figure 3 shows the projected, emission-weighted temperature map overlaid with the XSB contours. Often the X-ray temperature distribution provides the strongest constraints on the merger parameters. Two X-ray temperature maps have been published recently based on *ASCA* data (MFSV98; HDD99). Although largely consistent, they do differ systematically. Both maps show a similar degree of temperature variation (~ 6 -12 keV) within the cluster. However, the MFSV98 map shows a hot core with a radially decreasing temperature profile while the HDD99 map shows more of a temperature gradient across the cluster. The core is not the hottest region in the HDD99 map. For this reason, we have performed a region-by-region comparison of our model with both published temperature maps. Figure 4a is a comparison between our model and the corresponding regions in the MFSV98 map. Figure 4b compares the model temperatures within regions defined by HDD99 (see Fig. 3 for region definition). Our model agrees within the 90% confidence intervals of all but one region defined by MFSV98. In an absolute sense, the agreement with the HDD99 map is just as good although their quoted uncertainties are significantly smaller than those quoted by MFSV98. The most significant discrepancy between our model and HDD99 is in region 5 which includes the cluster core. Although our model agrees quite well with MFSV98 in this region (Region 1; Fig. 4a), the HDD99 map indicates a cooler core. If correct, this could be an indication that cooling may have started to influence the core (where cooling times are the shortest) because the merger is relatively old. Our current model does not include the effects of radiative cooling.

A3266 has recently been observed in the hard X-ray band (15-50 keV) by *BeppoSAX* (De Grandi & Molendi 1999). They found no evidence of a hard X-ray component nor is there currently any evidence of diffuse radio emission. This result is consistent with an old merger interpretation since shocks present in young mergers might be expected to accelerate relativistic particles which may produce observable diffuse radio emission via synchrotron and hard X-rays via inverse Compton scattering (see Sarazin 1999 for a recent review).

Given the model presented here, what can we say about the gas dynamics in A3266? First, A3266

appears to be an old off-axis merger in which the angular momentum of the initial clusters is due to tidal torquing (Flores et al. 1999). Previous off-axis merger simulations (Roettiger et al. 1998; Ricker 1998) have shown that mergers can transfer significant angular momentum to the ICM and that this angular momentum can be long-lived. In fact, because of the time and distance scales involved, it takes a considerable period (several billion years) for full rotation to develop. To understand this, consider a mean rotational velocity, $v_{rot}=1000 \text{ km s}^{-1}$, at a radius, $r=500 \text{ kpc}$. The time required to complete circulation about the core is then simply $t = 2\pi r/v_{rot}$ or $\sim 3 \text{ Gyr}$. In this model, full rotation occurs between 2.5 and 3 Gyr after core passage and persists beyond 4 Gyr. Of course this is in the absence of a second significant merger event which could potentially disrupt the circulation.

Figure 5 shows the gas velocities within an east-west plane taken along the observer's LOS and through the cluster core. Note that even at this late stage of the merger, there are still significant gas velocities ($>500 \text{ km s}^{-1}$) and that full rotation has been established. Further note, that shocks generated early in the merger have now dissipated while extremes in the temperature distribution have not. As we have pointed out previously (Roettiger et al. 1996), substructure of this type can persist well beyond the canonical sound crossing time. Thus, it may significantly influence estimates of cosmological parameters based on the frequency of substructure in clusters (e.g., Richstone, Loeb, & Turner 1992). As we will see in §3, our model not only predicts fully developed rotation in A3266, but also predicts a viewing geometry that places a significant component of the opposing bulk flows along the observer's LOS, thus enhancing the prospect of detecting it spectroscopically.

3. Observing the ICM Rotation with *Astro-E*

The *Astro-E* XRS (Audley et al. 1999) is a high resolution X-ray spectrometer scheduled for launch in early 2000. With $\sim 10 \text{ eV}$ energy resolution and a quantum efficiency near unity across the 0.4 to 10 keV energy band, it represents the first opportunity to directly observe gas dynamics in the ICM. Of course, these observations will be limited to LOS gas velocities, and will be confused by multiple temperature, velocity, and possibly metal abundance components along the LOS. For this reason, it is extremely useful

to have a 3-dimensional model of the gas density, temperature, and dynamical structure both when planning observations and interpreting the data.

Figure 6 represents a simple LOS emission-weighted mean velocity map based on the numerical model. Analogous to the temperature map (Fig. 3), velocities within a given computational zone along the LOS are simply weighted by the X-ray volume emissivity ($\propto n^2 T^{\frac{1}{2}}$). The range in velocities across the cluster is greater than 800 km s^{-1} . The opposing bulk motions evident on either side of the X-ray core constitute a strong signature of ICM rotation. West of the core, gas is moving away from the observer at greater than 500 km s^{-1} while east of the core, gas is moving toward the observer at greater than 300 km s^{-1} . Of course, this velocity map is only indicative of the observable LOS gas motions in the cluster. Below, we discuss detailed simulations of *Astro-E* observations.

Based on the model, we propose two pointings selected to optimize their expected velocity separation and XSB. We suggest one pointing on each side of the X-ray core, separated by $\sim 8'$ ($\sim 600 h_{70}^{-1}$) on an east-west line running $2'$ north of the X-ray maximum. The pointing location is chosen in part to avoid the point source located $\sim 4'$ due east of the core. The expected mean emissivity-weighted velocities at these two locations are -195 km s^{-1} (east) and $+533 \text{ km s}^{-1}$ (west) for a $\Delta V = 728 \text{ km s}^{-1}$.

In order to test the feasibility of this observation, we have used our numerical model and XSPEC (Arnaud 1996) to generate synthetic X-ray spectra for each of the two pointings described above. Each spectrum is a composite of 50 spectra (Raymond-Smith+absorption) characterized by the local ICM temperature, density, velocity, and chemical abundance within a computational zone along the observer's LOS. We have assumed a uniform abundance of 0.2 solar (De Grandi & Molendi 1999). The total flux of the simulated cluster is scaled to $2.84 \times 10^{-11} \text{ erg s}^{-1} \text{ cm}^{-2}$ (0.5-2.0 keV; David et al. 1999) while the absorption is characterized by $N_h = 3.0 \times 10^{20} \text{ cm}^{-2}$ (White et al. 1999). De Grandi & Molendi (1999) quote a somewhat lower absorption of $N_h = 1.6 \times 10^{20} \text{ cm}^{-2}$. Using the *ROSAT* PSPC image as a flux distribution template, a list of photon events is generated using MKPHLIST¹. Optimum exposures are determined to be 50 ksec (east) and 60 ksec (west). The resulting events were then input to

XRSSIM¹. After excluding photons not in the XRS FOV, the count rates for the east and west pointings are 0.20 and 0.17 cts s^{-1} , respectively, or approximately 10^4 counts per spectrum. After rebinning of the photons to improve the statistics, we produce the spectra shown in Fig. 7. An isothermal fit to the Fe K-line complex (6.2-6.7 keV) yields a velocity centroid shift of $-219 \pm 85 \text{ km s}^{-1}$ east of the core and $+544 \pm 80 \text{ km s}^{-1}$ west of the core for a velocity separation of $763 \pm 117 \text{ km s}^{-1}$ between the two pointings. These values are consistent with those expected from a direct examination of the numerical model (see above), thus demonstrating that the ICM rotation present in the model when scaled to the XSB of A3266 is in fact observable at a high level of significance with the *Astro-E* XRS.

4. Summary

We have presented a 3-dimensional numerical Hydro +N-body model of A3266 which is consistent with a wide range of observed properties. We believe A3266 represents an old ($\sim 3 \text{ Gyr}$), off-axis merger that is occurring into the plane of the sky at a 45° angle. The model is consistent, within resolution limits, with the *ROSAT* PSPC image, current *ASCA* temperature maps, *BeppoSAX* hard X-ray flux limits, the galaxy spatial and velocity distributions, and the existing radio data. We have also checked that the projected mass distribution agrees with gravitational lensing data.

In this model, the off-axis merger has imparted significant angular momentum on the ICM of the merger remnant which we predict should be observable with the XRS on *Astro-E*. The signature of rotation will appear as two opposing bulk flows ($\Delta V \sim 800 \text{ km s}^{-1}$) located on either side of the cluster's X-ray core along a line of constant declination. The degree of circulation present in the core of our model is consistent with high resolution Hydro+N-body simulations of galaxy cluster formation from cosmological initial conditions (Norman & Bryan 1998). Neither the galaxy redshift data nor the N-body particle distribution show similar evidence of rotation. Unlike the ICM interaction which can be characterized as 'collisional', the interaction between the subcluster galaxy components is 'collisionless'. Therefore, while the transfer of angular momentum between ICM components is very efficient, angular momentum is not transferred between the galaxy components.

¹<http://heasarc.gsfc.nasa.gov/docs/astroe/>

It is difficult to assess the overall uniqueness of our model at the present time. Individually, no single observation places a strong constraint on the model. Even taken together, there is considerable flexibility in the merger parameters and viewing geometry, and we cannot rule out the possibility that recent mergers with significantly less massive subclusters have played some role (HDD99). Although limitations in the current data set certainly contribute to this problem, it is also indicative of an older merger that no distinctive features currently exist. In the event ICM rotation is not detected, the observations described here will nonetheless provide important new constraints on the model and on ICM dynamics in general. In addition, these data will result in highly accurate temperature and metallicity measurements for two widely separated regions within a single cluster thus giving clues to the degree of spatial variation in both quantities. Inhomogeneities in the distribution of metals may help quantify the rate of mixing between gas components within the merger.

We would like to thank all the people who supported the *Astro-E* mission which inspired this work. We would also like to express our deep regret at the loss of the instrument during launch. We thank the Earth and Space Data Computing Division of NASA's Goddard Space Flight Center (GSFC) for use of the MasPar2 on which these simulations were performed. We also thank the Laboratory of High Energy Astrophysics at GSFC for making available the *ROSAT* archival data through the W3Browse facility and for making available the *Astro-E* simulation software. This work has made use of NASA's Astrophysics Data System (ADS) Abstract Service and the NASA/IPAC Extragalactic Database (NED). We thank J. P. Henry and J. O. Burns for their useful comments and discussions. The work of RF has been supported by a University of Missouri Research Board Award. KR dedicates this work to the memory of George O. Minot (1906-2000).

REFERENCES

- Arnaud, K. A. 1996, in ASP Conf. Ser. 101, *Astronomical Data Analysis Software and Systems*, eds. G. H. Jacoby & J. Barnes (San Francisco:ASP), 17
- Audley et al. 1999, *After the Dark Ages: When Galaxies were Young (the Universe at $2 < z < 5$)*, eds. S. Holt & E. Smith. AIP, 428
- Barnes, J. E., & Efstathiou, G. 1987, *ApJ*, 319, 575
- Bekki, K. 1999, *ApJ*, 510, L15
- Birkinshaw, M. 1999, *Physics Reports*, 310, 97
- Burns, J. O., 1998, *Science*, 280, 345
- Burns, J. O., Roettiger, K., Ledlow, M., & Klypin, A. 1994, *ApJ*, 427, L87
- Colella, P. & Woodward, P. 1984, *J. Comp. Phys.*, 54, 174
- David, L. P., Forman, W., & Jones, C. 1999, *ApJ*, 519, 1999
- De Grandi, S. & Molendi, S. 1999, *ApJ Letters*, in press. (astro-ph/9910413)
- Dressler, A. & Gunn, J. E. 1983, *ApJ*, 270, 7
- Flores, R., Quintana, H., & Way, M. J. 1999, *ApJ*, in press. (astro-ph/9903292)
- Fujita, Y., Takizawa, M., Nagashima, M., & Enoki, M. 1999, *PASJ*, 51, L1
- Gomez, P., Loken, C., Roettiger, K., & Burns, J. O. 1999, *ApJ* submitted.
- Henriksen, M., Donnelly, R. H., & Davis, D. S. 1999, *ApJ*, in press (astro-ph/9909243) (HDD99)
- Inagaki, Y., Sugimotohara, T., & Suto, Y. 1995, *PASJ*, 47, 411
- Joffe, M. et al. 1999, submitted to ASP Conf. Ser., *Gravitational Lensing: Recent Progress and Future Goals*, eds T. Brainerd and C. Kochanek (astro-ph/9909029)
- Jones, P. A. & McAdam, W. B. 1992, *ApJS*, 80, 137
- Kravtsov, A. V., & Klypin, A. A. 1998, in the *Proceedings of the 12th Potsdam Cosmology Workshop, Large Scale Structure: Tracks and Traces*. Eds. V. Mueller, S. Gottloeber, J. P. Muecket, J. Wambsganss. World Scientific, 31
- Markevitch, M., Forman, W. R., Sarazin, C. L. & Vikhlinin, A. 1998, *ApJ*, 503, 77 (MFSV98)
- McGlynn, T. A. & Fabian, A. C. 1984, *MNRAS*, *ApJ*, 208, 709
- Mohr, J. J., Fabricant, D. G., & Geller, M. J. 1993, *ApJ*, 413, 492
- Mohr, J. J., Mathiesen, B. & Evrard, A. 1999, *ApJ*, 517, 627
- Moore, B., Katz, N., Lake, G., Dressler, A., & Oemler, A. Jr. 1996, *Nature*, 379, 613

- Norman, M. L. & Bryan, G. L. 1998, in Ringberg Workshop on M87, eds. K. Meisenheimer & H.-J. Röser, Springer Lecture Notes in Physics (astro-ph/9802335)
- Peebles, P. J. E. 1969, ApJ, 155, 393
- Peres, C. B. et al. 1998, MNRAS, 298, 416
- Quintana, H., Ramirez, A., & Way, M. J. 1996, AJ, 112, 36
- Richstone, D., Loeb, A. & Turner, E. L. 1992, ApJ, 393, 477
- Ricker, P. M., 1998, ApJ, 496, 670
- Roettiger, K., Burns, J. O., & Loken, C. 1996, ApJ, 473, 651
- Roettiger, K., Stone, J. M., & Mushotzky, R. 1997, ApJ, 482, 588
- Roettiger, K., Stone, J. M., & Mushotzky, R. 1998, ApJ, 493, 62
- Roettiger, K., Burns, J. O., & Stone, J. M. 1999, ApJ, 518, 603
- Sarazin, C. 1999, ApJ, 520, 529
- White, D. A., Jones, C., & Forman, W. 1999, MNRAS, 292, 419

Fig. 1.— The *ROSAT* PSPC archival image of Abell 3266. The image is background subtracted. Contour levels are 0.02, 0.04, 0.07, 0.14, 0.25, 0.45, 0.55, 0.65, 0.75, 0.85, 0.95 of peak.

Fig. 2.— A synthetic X-ray surface brightness image generated from the numerical model of A3266. Contours and linear dimensions (assuming $H_0 = 70 \text{ km s}^{-1} \text{ Mpc}^{-1}$) are the same as in Fig. 1. The \diamond 's and + 's represent primary and secondary cluster particles, respectively.

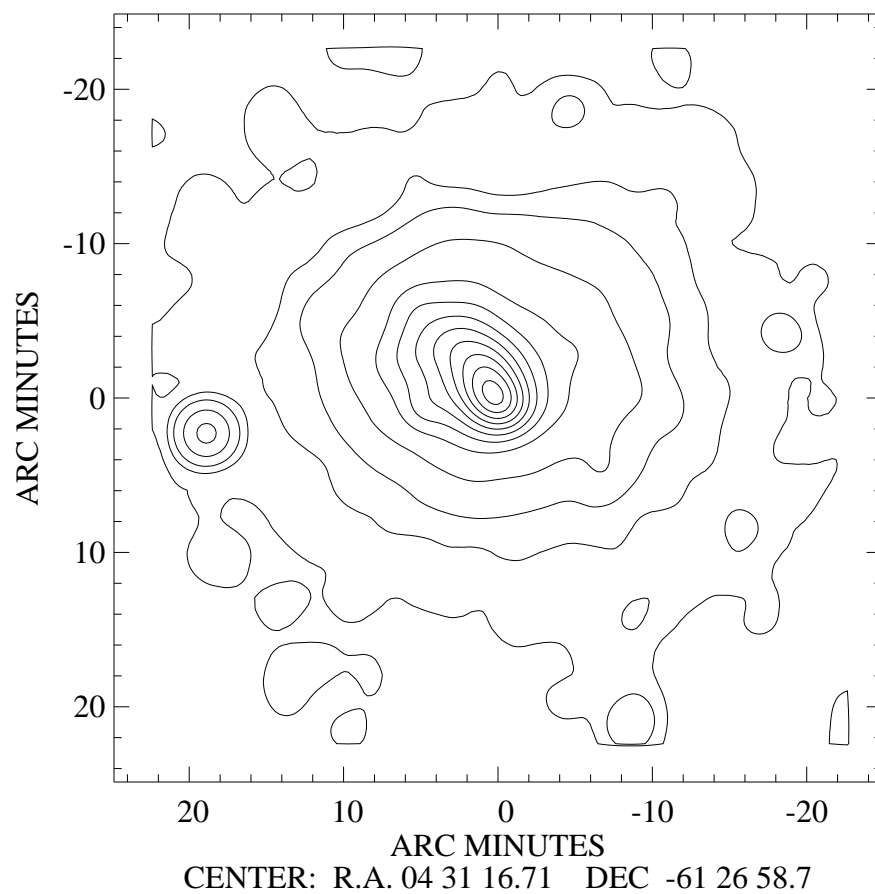
Fig. 3.— The projected emission-weighted temperature map of the A3266 model (color) overlaid with the X-ray surface brightness (contours). The numbered boxes are the temperature regions defined by HDD99.

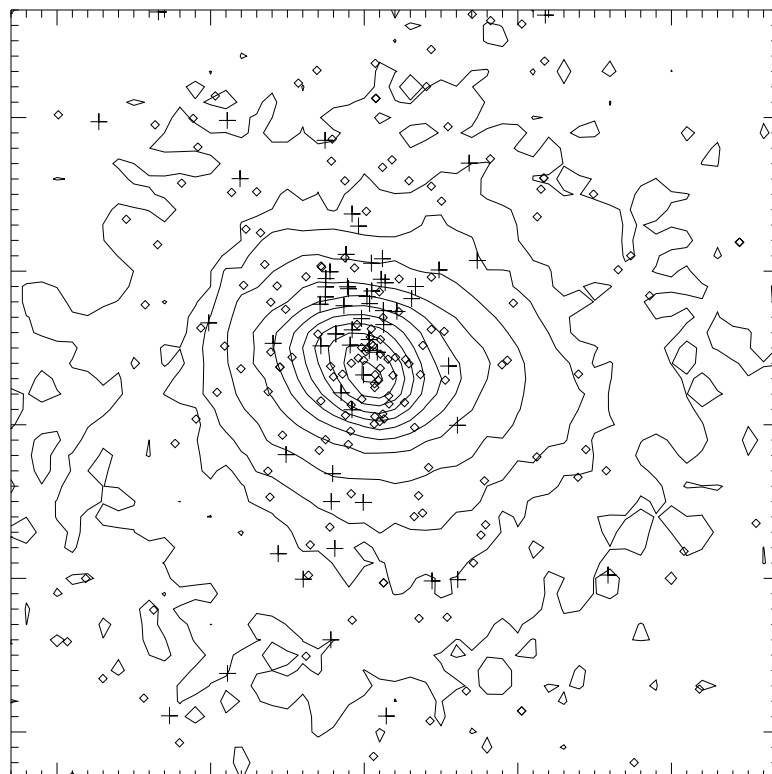
Fig. 4.— Region-by-Region comparisons between the model temperature distribution and that observed by a) MFSV99 and b) HDD99 using *ASCA*. The regions defined by HDD99 are shown in Fig. 3.

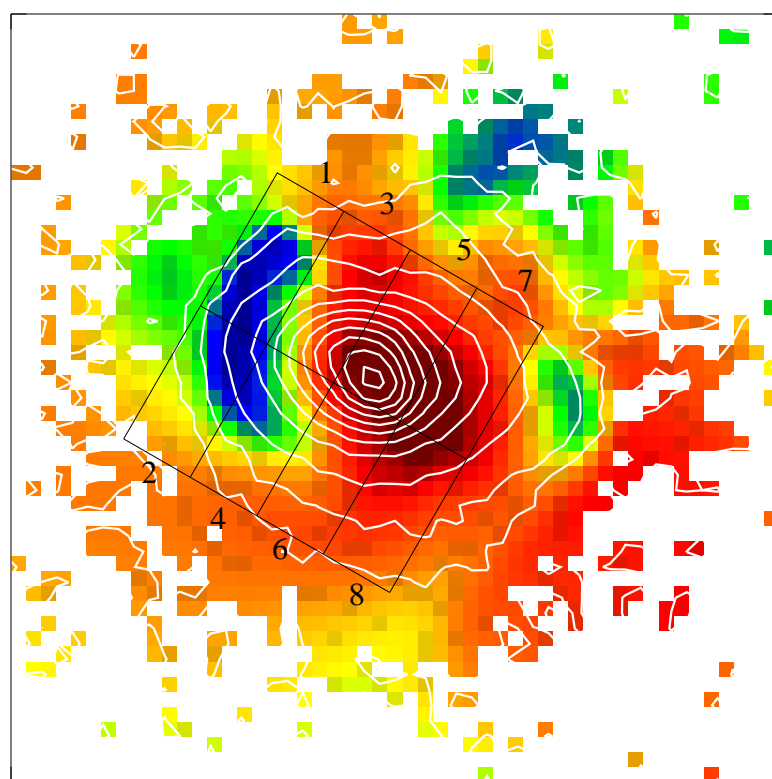
Fig. 5.— Velocity vectors overlaid with X-ray emissivity (contours) within a 2-dimensional east-west (left to right) slice taken through the cluster core and along the observer's LOS (bottom to top). Note the large-scale counterclockwise rotation near the cluster core. Panel dimensions are $3.3 \times 3.3 \text{ Mpc}$. The longest vector is $\sim 900 \text{ km s}^{-1}$.

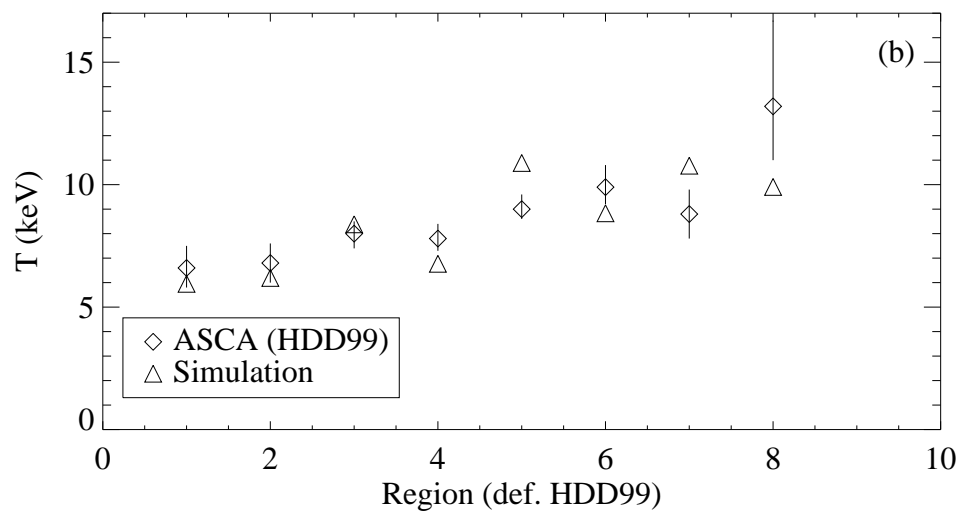
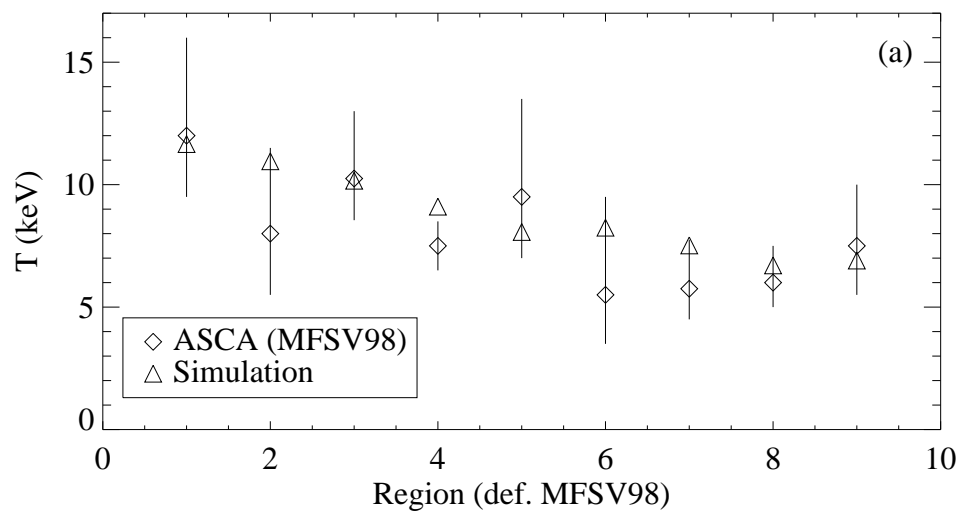
Fig. 6.— Emission-weighted LOS ICM velocities (color) overlaid with X-ray surface brightness (contours). Velocities on the eastern half of the cluster (blue) are moving toward the observer while velocities on the western half of the cluster (red) are moving away from the observer. The background color (light blue) corresponds to 0 km s^{-1} .

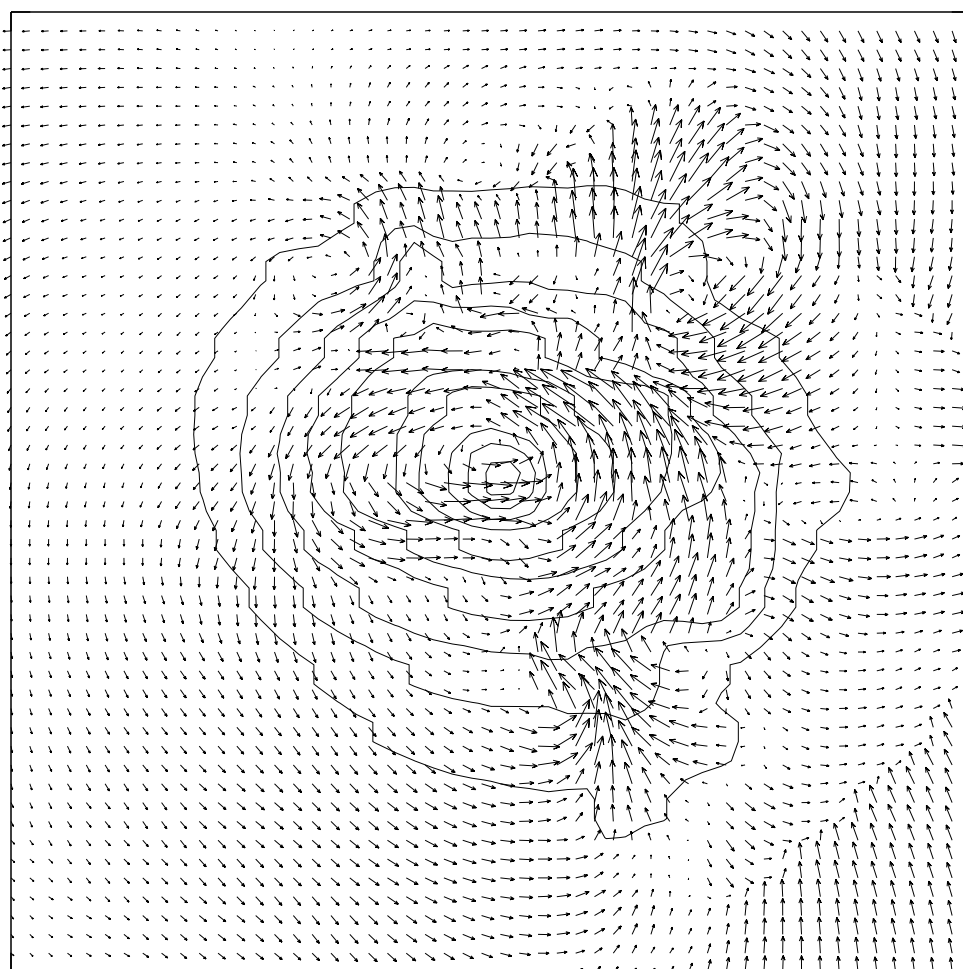
Fig. 7.— Simulated *Astro-E* spectra taken $4'$ on either side the X-ray core along an East-West line $2'$ north of the core. Each represents a 50-component model (ρ, T, v from 50 zones within the numerical simulation) normalized to the flux at the corresponding location in A3266. The vertical solid lines indicate the location of the fit to the line centroid. Integration times are 50 ksec East and 60 ksec West.

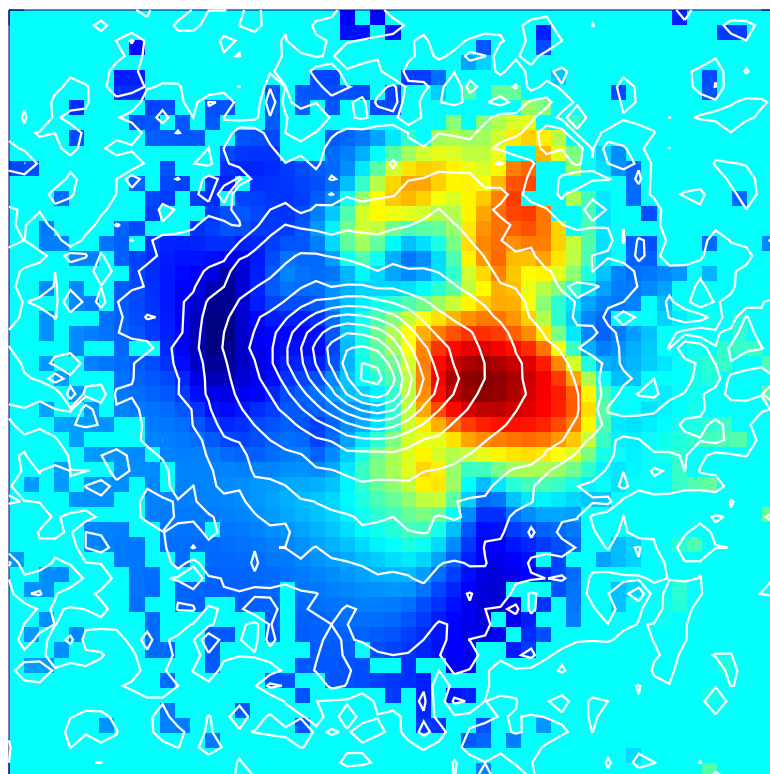












-370 km s⁻¹

+580 km s⁻¹

